The crystal structure and electronic properties of perovskite-type RMnO$_3$(R = Ho ~ Lu)

○Tomotaka Shimoyama[a], Makoto Tachibana[b], Hitoshi Kawaji[a], Tooru Atake[a], Yoshihiro, Kuroiwa[c]

[a] *Materials and Structures Laboratory, Tokyo Institute of Technology*

[b] *National Institute for Materials Science*

[c] *Graduate School of Science, Hiroshima University*

Name: Tomotaka Shimoyama

Grade: Third -year of doctoral course

Proposal Number: 2007A1824

Beamline: BL02B2

Introduction

Perovskite manganites RMnO$_3$ (R = rare earth) have been attracting much attention because of their unusual states arising from the subtle interplay among charge, spin, orbital, and lattice degrees of freedom. Colossal magnetoresistance and charge ordering in hole-doped LaMnO$_3$ have been the subjects of great interest for the last decade [1], while recent discoveries of multiferroicity in TbMnO$_3$ [2] and DyMnO$_3$ [3] have stimulated additional attention in the studies of manganites. These electronic behaviors are all strongly dependent on the underlying lattice, and detailed knowledge on the properties and structure concerning with R is expected to provide significant insights into the complex physics of manganites. So far, Kimura *et al.* [4] have explained that there is complex magnetic transition on RMnO$_3$ (R = La ~ Ho) below 100 K. And we completed the magnetic phase diagram for RMnO$_3$ (R = La ~ Lu) as a function of r_R and temperature is obtained as shown in Fig. 1 from the heat capacity measurement for RMnO$_3$ (R = Ho ~ Lu). The phase boundary for paramagnetic phase shows smooth variations with r_R. However, the boundaries are new steep for separating the A-type, spiral, and E-type AF phases at low temperatures.

In addition, Kimura *et al*. invoked the competition between nearest-neighbor (NN) FM interaction and next-nearest-neighbor (NNN) AF interaction [5] in the *ab* plane to explain the phase diagram.

On the other hand, Zhou and Goodenough [6] have recently reported the T_N and the crystal structure for the entire series of R (R = La-Lu), and concluded that there should be relevant competition between FM e_g-O-e_g and AF t_{2g}-O-t_{2g} interactions in the *ab* plane, rather than the AF NNN interaction as proposed by Kimura et al[4].

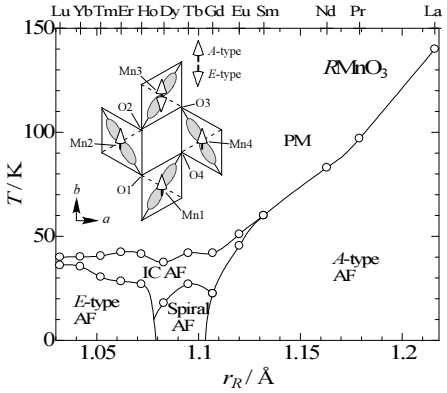

Fig. 1. Magnetic phase diagram for RMnO$_3$ as a function of the ionic radius of R (r_R). Published data [1] are used for R = La ~ Dy. Inset shows a sketch of the MnO$_2$ framework, d_{3x2-r2}/d_{3y2-r2} orbitals, and spin-order in the *ab* plane. The orbitals are located along the (*l*) Mn-O bonds, while dashed lines represent the short (s) Mn-O bonds. Orbital and spin-order are uniform and staggered, respectively, along the *c* axis.

Moreover, they argued [6] that the JT distortion plaied the dominant role in determining T_N, and both the JT distortion and T_N become insensitive to a change in r_R for R = Ho ~ Lu with the E-type structure. Further studies are needed to evaluate these conflicting ideas, and more detailed experiments for R = Ho ~ Lu are in order before additional theories are put forth: The expected IC phase does not appear in Ref. 6, and the large scatter in the reported structural parameters [6, 7] may lead to misleading interpretations.

We made high-quality samples prepared by the high-pressure technique. Our synchrotron X-ray powder diffraction study revealed the significant increase of JT distortion for the smallest R compound, providing important perspectives for understanding the complex phase diagram of RMnO$_3$.

Experiment

Polycrystalline samples of perovskite RMnO$_3$ (R = Ho, Er, Tm, Yb, and Lu) were prepared under high pressure. First, pure samples of hexagonal RMnO$_3$ were obtained from R_2O_3 and Mn_2O_3 by solid-state reactions in air. The powders were then sealed in gold capsules and heated to 1573 K for 60 min at 6 GPa in a belt-type press, and then rapidly cooled to room temperature before releasing the pressure.The heat capacity was measured from 2 K to 60 K by using a relaxation calorimeter (PPMS, Quantum Design Inc.). The powder X-ray diffraction measurements with synchrotron radiation were carried out at the BL02B2 beam line of SPring-8 of Japan Synchrotron Radiation Research Institute (JASRI) with a wavelength of λ = 0.41509 Å.

Results and Discussion

Structural parameters were refined by Rietveld method, using the program RIETAN-2000 [8]. Good reliability factors were obtained in each case. The Rietveld refinement pattern for R = Ho is plotted in Fig. 2. The refined structural parameters for R = Ho ~ Lu are tabulated in Table 1.

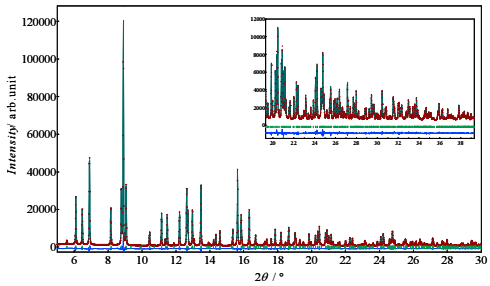

Fig.2. Results of synchrotron X-ray powder diffraction patterns for HoMnO$_3$. Bragg reflections are indicated by tick marks. Inset shows the high angular region in an enlarged scale.

Figure 3 displays the variation of the lattice parameters a, b, and c, and various Mn-O-Mn bond angles and Mn-O bond distances (long "l", medium "m", short "s") as a function of r_R. The present results for R = Ho ~ Lu join smoothly with the reported data [9 - 11] for larger R, expect for those of [6]. The present data are precise enough to be used in subsequent analysis without imposing any guiding fits. Both a and c axes show continuous decrease with decreasing r_R, while b axis shows a broad maximum around interme diate r_R. These behaviors as well as the relation $c/\sqrt{2} < a$ [12, 13], concur with the evolution of the octahedral rotation and JT distortion (described in the next patagraph). While m and <Mn-O> become r_R independent below ~1.13 Å, there is significant increase in l and decrease in s for r_R ~1.07 Å. The increase in l is opposite to what was claimed in Ref.6, though *not* inconsistent with its actual data [12]. This correction has important consequences on the understanding of the JT distortion.

Table 1. Lattice parameters (Å), atomic coordinates [R 4c (x, y, 1/4); Mn 4b (0, 1/2, 0); O_I 4c (x, y, 1/4); O_{II} 8d (x, y, z)], atomic displacement parameters (Å^2), reliability factors, and selected bond distance (Å) and bond angles (°) for RMnO$_3$ (R = Ho - Lu).

R	Ho	Er	Tm	Yb	Lu
a	5.2395(1)	5.2395(1)	5.2277(1)	5.2395(1)	5.2395(1)
b	5.8223(1)	5.8223(1)	5.8085(1)	5.8223(1)	5.8223(1)
c	7.3357(1)	7.3357(1)	7.3175(2)	7.3357(1)	7.3357(1)
x (R)	0.98215(8)	0.98215(8)	0.98217(9)	0.98215(8)	0.98215(8)
y (R)	0.08437(6)	0.08437(6)	0.08450(7)	0.08437(6)	0.08437(6)
B (R)	0.487(9)	0.487(9)	0.590(10)	0.487(9)	0.487(9)
B (Mn)	0.487(9)	0.37(2)	0.45(2)	0.487(9)	0.487(9)
x (O_I)	0.37(2)	0.1138(9)	0.1147(10)	0.37(2)	0.37(2)
y (O_I)	0.1138(9)	0.4607(9)	0.4591(10)	0.1138(9)	0.1138(9)
B (O_I)	0.61(10)	0.61(10)	0.70(12)	0.61(10)	0.61(10)
x (O_{II})	0.6997(7)	0.6997(7)	0.6984(8)	0.6997(7)	0.6997(7)
y (O_{II})	0.3343(7)	0.3343(7)	0.3372(8)	0.3343(7)	0.3343(7)
z (O_{II})	0.0563(4)	0.0563(4)	0.0571(5)	0.0563(4)	0.0563(4)
B (O_{II})	0.71(8)	0.71(8)	0.83(10)	0.71(8)	0.71(8)
R_{wp}(%)	3.89	3.89	4.00	3.89	3.89
R_I(%)	2.00	2.00	2.56	2.00	2.00
S	1.72	1.72	1.69	1.72	1.72
Mn-O_I (×2,m)	1.942(2)	1.942(2)	1.940(2)	1.942(2)	1.942(2)
Mn-O_{II} (×2,l)	2.248(4)	2.248(4)	2.255(5)	2.248(4)	2.248(4)
Mn-O_{II} (×2,s)	1.891(4)	1.891(4)	1.886(4)	1.891(4)	1.891(4)
<Mn – O>	2.027	2.027	2.027	2.027	2.027
Mn - O_I - Mn	141.59(2)	141.59(2)	141.15(2)	141.59(2)	141.59(2)
Mn- O_{II}- Mn (2)	142.05(5)	142.05(5)	142.17(5)	142.05(5)	142.05(5)

The JT distortion for each R compound can be evaluated from l, m, and s, and the results are summarized in Fig. 4. The Q_2 and Q_3 are the orthorhombic and tetragonal distortion modes of MnO_6 octahedra, respectively, and they form orthogonal axes in the (Q_2, Q_3) plane to lead to the potential surface of distortion [6, 15]. Here, ρ_0 is a radius in the plane that corresponds to the magnitude of the JT distortion. As the octahedral rotation is superposed on the cooperative JT distortion, the staggered distortion has two minima in the (Q_2, Q_3) plane with a negative Q_3 and an angle ϕ from the positive and negative Q_2 axes [6, 15]. The Q_2 increases with decreasing r_R, and shows plateau region at intermediate r_R. The magnitude of Q_3 also increases with decreasing r_R, but levels off below r_R ~1.12 Å. Consequently, ρ_0 evolves in a manner similar to Q_2, with a plateau in the same region. The ϕ shows a maximum as reported in Ref. 6, but the present results show that the decrease in ϕ below $r_R \sim 1.10$ Å is due to the increase in Q_2, rather than a decrease in $|Q_3|$ [6]. The maximum in ϕ, as well as the plateaus in Q_2 and ρ_0 and the curvature of Mn-O_{II}-Mn bond angle all correspond closely to the broad maximum in b, which in turn originates from the intrinsic geometric property of the orthorhombic perovskites [12]. As a result of this crystallographic feature, the reduction in r_R initially increases both the Q_2 and Q_3 distortion modes, but then the distortion is saturated around $r_R \sim$ 1.13–1.08 Å. Further decrease in r_R reaches the region where b decreases significanly, where the strong elongation of the MnO_6 octahedra in the ab plane and significant increase in the Q_2 mode takes place.

The revised structural parameters provide significant implications for the model proposed in Ref. 6. First, the increase in JT distortion for the smallest R compound implies that the energy splitting of the e_g orbitals continues to increase with decreasing r_R, so R = Lu should have the largest charge gap [6] with the weakest FM exchange interaction. Moreover, it is not immediately obvious how the competition involving

a single exchange path leads to the observed IC structure. On the other hand, competition with the NNN interaction [4] would explain the phase diagram, since it predicts the IC structure to evolve into the highly distorted members of RMnO$_3$. The fact that T_N does not decrease with decreasing r_R implies that the NNN AF interaction becomes increasingly important. Indeed, the model [4] predicts that the strength of NNN interaction along the b axis increases faster than the decrease in NN FM interaction for the Mn-O-Mn bond angles from ~145° to ~130°, which would explain the small change in T_N for small r_R. The increasing importance of the NNN interaction is also supported by the O2-O4 distance, which is shown in Fig. 4. Due to the increased rotation of the MnO$_6$ octahedra, O2-O4 decreases continuously from 3.40 Å for R = La to 2.89 Å for R = Lu.

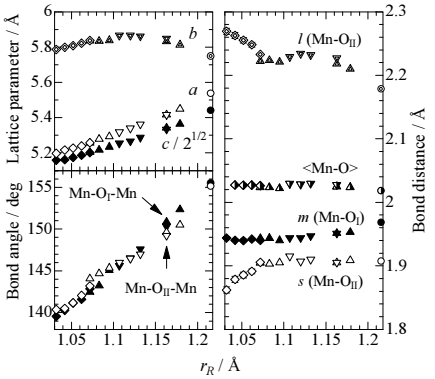

Fig.3. Variation of the lattice parameters, Mn-O-Mn bond angles, and Mn-O bond distance as a function of r_R. O_{II} is in the ab plane(O1-O4 in Fig.2), while O_I is at the apical position along the c axis. Sources: circle, Ref.3; triangle, Ref.4; inverted triangle, Ref.5; diamond, this study. Data for R = Y and Er from Ref.4 are not shown because the samples are nonstoichiometric. The error bars are shown for our results when they are larger than the

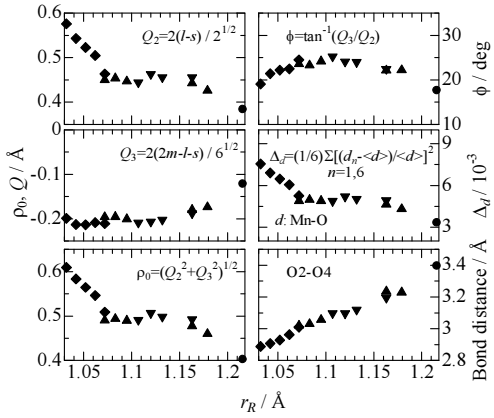

Fig.4. Evolution of the various parameters associated with JT distortion, and the O2-O4 distance, as a function of r_R. Symbols are the same as in Fig.3.

Conclusion

In contrast to the previous report [6], the present study reveals the siginificant increase of JT distortion for smaller R compounds, and provides additional support for the importance of NNN interaction. Further theories incorporationg both the NNN interaction and JT distortion are expected to provide better understanding of the phase diagram.

References

[1] *Colossal Magnetoresistive Oxides*, edited by Y. Tokura (Gordon and Breach, London, 2000).

[2] T. Kimura, T. Goto, H. Shintani, K. Ishizaka, T. Arima, and Y. Tokura, Nature (London) **426**,55 (2003).

[3] T. Goto, T. Kimura, G. Lawes, A. P. Ramirez, and Y. Tokura, Phys. Rev. Lett. **92**, 257201 (2004)

[4] T. Kimura, S. Ishihara, H. Shintani, T. Arima, K. T. Takahashi, K. Ishizaka, and Y. Tokura, Phys. Rev. B **68**, 060403(R) (2003).

[5]A. Muñoz, M. T. Casáis, J. A. Alonso, M. J. Martínez-Lope, J. L. Martínez, M. T. Fernández-Díaz, Inorg. Chem. **40**, 1020 (2001).

[6] J.-S. Zhou and J. B. Goodenough, Phys. Rev. Lett. **96**, 247202 (2006).

[7] J.-S. Zhou, J. B. Goodenough, J. M. Gallardo-Amores, E. Morán, M. A. Alario-Franco, and R. Caudillo, Phys. Rev. B **74**, 014422 (2006).

[8] F. Izumi and T. Ikeda, Mater. Sci. Forum **321-324**, 198 (2000).

[9] J. Rodríguez-Carvajal, M. Hennion, F. Moussa, A. H. Moudden, L. Pinsard, and A. Revcolevschi, Phys. Rev. B **57**, R3189 (1998).

[10] J. A. Alonso, M. J. Martínez-Lope, M. T. Casais, and M. T. Fernández-Díaz, Inorg. Chem. **39**, 917 (2000).

[11] T. Mori, N. Kamegashira, K. Aoki, T. Shishido, and T. Fukuda, Mater. Lett. **54**, 238 (2002).

[12] J.-S. Zhou and J. B. Goodenough, Phys. Rev. Lett. **94**, 065501 (2005).

[13] M. W. Lufaso and P. M. Woodward, Acta Crystallogr., Sect. B: Struct. Sci. **60**,10 (2004).

[14] Reference 6 assumed constant m and decreasing l and s for r_R ~1.10 Å, which is not consistent with its data for <Mn-O> that increases slightly with decreasing r_R.

[15] J. Kanamori, J. Appl. Phys. **31**, S14 (1960)